JOURNAL OF MATERIALS SCIENCE 30 (1995) 5281–5286

Effects of residual stress on toughening of brittle polycrystals

D. K. M. SHUM
Saint-Gobain/Norton Industrial Ceramics Corporation, Goddard Road, Northboro, MA 01532, USA

The effects of residual stress on toughening of brittle polycrystalline materials, in the absence of microcracking, were investigated by considering the mode I stress intensity factor reduction at the tip of a stationary crack under combined applied and residual stress loading. Toughness enhancement associated with a number of model singular and non-singular residual stress fields was evaluated. The singular residual stress fields were used to model grain-sized thermal expansion anisotropy due to grain-orientation differences in a polycrystal. The numerical results indicate that residual stress can significantly toughen a stationary crack against initiation. For the same average value of residual stress, toughness enhancement due to singular residual stress fields is more substantial than that due to non-singular residual stress fields. Sample toughness enhancement results are presented for a single-phase polycrystal failing by intergranular fracture.

1. Introduction

It is well known that residual stress develops in some brittle polycrystalline materials as a consequence of grain-sized thermal expansion anisotropy. Release of residual stress with profuse microcracking serves to toughen the microcracked polycrystals, and this toughening mechanism has received much attention [1–5]. However, residual stress is also believed to play a part in determining the fracture toughness of brittle polycrystals where profuse microcracking is not observed. This work examined the effects of residual stress on toughening of brittle polycrystalline materials in the absence of microcracking. Specifically, the study considered the mode I stress intensity factor reduction at the tip of a stationary crack under combined applied and residual stress loading. Toughness enhancement associated with a number of singular and non-singular periodic residual stress fields was examined. The singular residual stress fields were then used to model the (theoretically) singular stress distribution along grain boundaries of a polycrystal resulting from grain-sized thermal expansion anisotropy due to grain-orientation differences [6]. The stress intensity factor reduction results obtained from this study, though highly idealized, are believed to offer insights into the maximum amount of toughening achievable with residual stress in brittle polycrystals.

2. Crack-tip stress intensity reduction

A continuum approach was taken in this study in which a polycrystalline material is treated as being linear elastic, homogeneous and isotropic on a macroscale. Attention is focused on the fracture problem in which a crack with length much larger than the average grain size exists within the polycrystal. Consistent with the stated length-scale assumption, the fracture behaviour of this material is modelled by considering the asymptotic plane problem of an infinite solid with a semi-infinite crack along the negative x-axis, as shown in Fig. 1, where the semi-infinite crack is remotely stressed consistent with the classic mode I crack-tip field of the form

$$\sigma_{\alpha\beta} = \frac{K^{\infty}}{(2\pi r)^{1/2}} \tilde{\sigma}_{\alpha\beta}(\theta) \tag{1}$$

where (r, θ) are planar polar coordinates.

A periodic, self-equilibrating residual stress field representative of grain-sized thermal-expansion anisotropy due to grain-orientation differences is assumed to exist within this polycrystal. This study is highly idealized in that the residual stress field is modelled to be one-dimensional in nature with a period of length $2L$. Over each period the residual stress distribution has the form

$$\sigma(x) = \sigma_0 f(x) \qquad 0 \leq x < 2L \tag{2}$$

where σ_0 is a reference residual stress to be specified shortly. Zero average residual stress over each period of length $2L$ is guaranteed by requiring the residual stress field to obey the relation

$$f(x) = -f(2L - x) \qquad 0 \leq x < L \tag{3}$$

The residual stress field is aligned with the semi-infinite crack as shown in Fig. 2 such that, in the absence of external loads, a traction distribution, $\sigma(x)$, of the

0022–2461

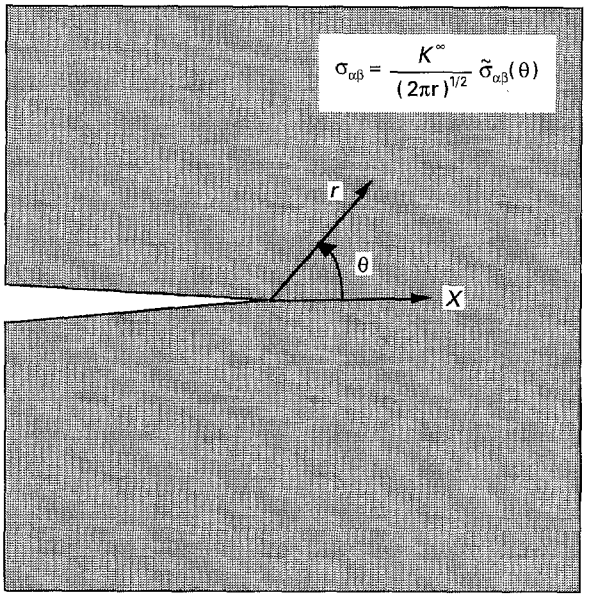

Figure 1 Semi-infinite crack geometry.

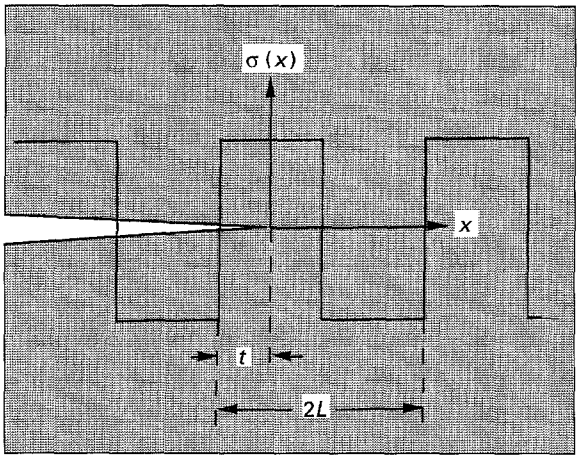

Figure 2 Schematic drawing of a square wave residual stress distribution prior to the introduction of the semi-infinite crack.

form in Equations 2 and 3 exists along the entire x-axis of the infinite body *prior* to the introduction of the semi-infinite crack. Location of the semi-infinite crack tip with respect to the periodicity of the residual stress field is denoted by the distance variable, t, where $0 \leq t < 2L$.

Using linear superposition, the mode I stress intensity factor, K_t at the semi-infinite crack tip under combined applied and residual stress loading takes the form

$$K_t = K^\infty + K_r \tag{4}$$

where K_r represents the stress intensity factor contribution due to the traction distribution, $\sigma(x)$, in the material through which the crack has passed. From Equation 4 it is clear that shielding of the semi-infinite crack is possible only if the release of residual stress in the material, through which the crack has passed, results in a negative K_r contribution to the crack tip. In this sense the effect of residual stress on toughening of a brittle polycrystal is a crack-wake phenomenon. From dimensional considerations, K_r has the form

$$K_r = \sigma_0 L^{1/2} g\left(\frac{t}{L}\right) \tag{5}$$

where $g(t/L)$ represents the variation of K_r as a function of the normalized crack-tip location, t/L, and the residual stress distribution, $f(x)$. With reference to Fig. 2, the function $g(t/L)$ takes the form [7]

$$g\left(\frac{t}{L}\right) = \left(\frac{2}{\pi}\right)^{1/2} \left\{ \int_0^{t/L} \frac{f[1 + u - (t/L)]}{u^{1/2}}\, du + \int_0^\infty \frac{f(1+u)}{[u + (t/L)]^{1/2}}\, du \right\} \tag{6}$$

Toughness enhancement is associated with the range of crack-tip locations for which the function $g(t/L)$ is negative, and maximum toughening occurs when $g(t/L)$ reaches a minimum. Because the residual stress distribution expressed in Equation 2 is periodic over a distance of length $2L$, determination of K_r as a function of crack-tip position can be limited to the range $0 \leq t/L < 2$. The case of $t/L = 0$ corresponds to the geometry where the tip of the semi-infinite crack is about to enter a region under residual tension.

Introduce the toughening ratio, Λ, by rewriting Equation 4 such that

$$\Lambda = \frac{K^\infty}{K_t} = 1 - \frac{\sigma_0 L^{1/2}}{K_t} g(t/L) \tag{7}$$

where Λ is the ratio of the magnitude of the applied stress intensity factor, K^∞, to the crack-tip stress intensity factor, K_t. In the following section, toughness enhancement due to residual stress fields of various forms is examined, and the function $g(t/L)$ associated with each residual stress field is determined. The toughening achievable with the various residual stress fields for a specific polycrystal can, in principle, be determined by evaluating the toughening ratio, Λ, with K_t identified with the intrinsic toughness, K_m, of the polycrystal. The function $g(t/L)$ is referred to as the unit function in subsequent discussions, corresponding to the toughening contribution when the non-dimensional residual stress parameter, $\sigma_0 L^{1/2}/K_m$, has the value of unity.

3. Candidate residual stress fields

The periodicity of the residual stress field in Equation 2 corresponds to the minimum distance over which positive and negative residual stresses of a self-equilibrating residual stress field cancel, and is of the order of a few grain diameters in polycrystals with random grain orientation. Expressed in terms of the normalized distance $u = x/L$, the spatial distribution function, $f(u)$, in Equation 2 for the residual stress fields examined in this study, over the range $0 \leq u \leq 1$, are shown in Fig. 3 and have the following explicit forms

sine wave

$$f(u) = \frac{\pi}{2} \sin(\pi u) \tag{8a}$$

square wave

$$f(u) = 1 \tag{8b}$$

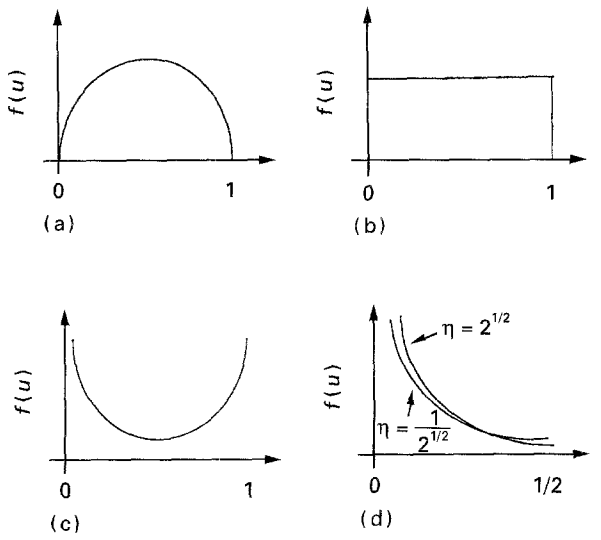

Figure 3 Schematic drawings of the various residual stress fields over one-half period: (a) sine wave, (b) square wave, (c) algebraically singular, (d) logarithmically singular. Explicit equations for these residual stress fields can be found in Equations 8a–e in the text.

algebraically singular

$$f(u) = \frac{\gamma}{[1-(2u-1)]^{\varepsilon}} \qquad \left(0 < \varepsilon < \frac{1}{2}\right) \tag{8c}$$

logarithmically singular

$$f(u) = \left(\frac{3}{2}Au + B\right)\ln\left[\left(\frac{3}{2}\right)^2 u(1-u)\right]$$

$$\left(0 \le u \le \frac{1}{2}\right) \tag{8d}$$

$$f(u) = f(1-u) \qquad \left(\frac{1}{2} \le u \le 1\right) \tag{8e}$$

$$A = 0.560, \quad B = -0.478, \quad \text{for } \eta = 2^{1/2},$$

$$A = -0.264, \quad B = -0.396, \quad \text{for } \eta = 1/2^{1/2}$$

The sine wave in Fig. 3a is used to model a smoothly varying residual stress field. In Fig. 3b the square wave is used to model a discontinuous but finite-valued residual stress field. A general singular residual stress field is modelled using an algebraically singular field as shown in Fig. 3c. The parameter, ε, in Equation 8c can be adjusted to model varying degrees of singularity, while the parameter, γ, is used to facilitate comparison of results based on different values of the parameter, ε, in a manner soon to be apparent. Finally, two logarithmically singular residual stress fields characterized by an elastic anisotropy factor, η, are shown in Fig. 3d. These two logarithmically singular fields are of particular interest because they represent a wide range of elastic anisotropy mismatches within individual grains in polycrystalline ceramics [6]. Tvergaard and Hutchinson's analysis [6] was performed for an idealized hexagonal polycrystal, and details concerning the elastic anisotropy factor, η, can be found in that work. The empirical constants A and B are found from curve-fitting the results in [6] to the form shown in Equations 8d and e. The periodicity of the logarithmically singular residual stress fields in [6] is three facet lengths of the hexagonal grains, and is identified with $2L$ in this study.

Comparison of crack-shielding capability of the various residual stress fields, based on equal values of the average residual stress over each half-period, is accomplished by requiring the residual stress fields to obey the relation

$$\int_0^1 f(u)\,du = 1 \tag{9}$$

The reference residual stress value, σ_0, in Equation 2 thus corresponds to the magnitude of the average residual stress experienced in each half-period. Equation 9 is satisfied by the non-singular sine and square wave residual stress fields shown in Equations 8a and b. For the algebraically singular residual stress fields the parameter pair (γ, ε) are chosen such that Equation 9 is also satisfied. On the other hand, curve-fitting of the results in [6] to the logarithmically singular form in Equations 8d and e for the two cases of elastic anisotropy in Equation 8 results in relations of the form

$$\int_0^1 f(u)\,du = 0.4 \qquad \text{for } \eta = 2^{1/2} \tag{10a}$$

$$\int_0^1 f(u)\,du = 0.55 \qquad \text{for } \eta = \frac{1}{2^{1/2}} \tag{10b}$$

In presenting toughness enhancement results in the next section, the logarithmically singular results will be shown for values of the integral expression indicated in Equations 10a and b, and for values of the integral expression equal to unity so that comparison with other residual stress field results can be made.

Determination of the numerical accuracy in evaluating the unit-function $g(t/L)$ in Equation 6 is facilitated by the following two check cases. For the sine wave residual stress field, $g(t/L)$ can be evaluated in closed-form such that

$$g\left(\frac{t}{L}\right) = \frac{1}{\pi^{1/2}}\left[\cos\left(\pi\frac{t}{L}\right) - \sin\left(\pi\frac{t}{L}\right)\right] \tag{11}$$

For the case where the singularity parameter, ε, of the algebraically singular residual stress field approaches zero, the toughness enhancement results based on Equation 9 should coincide with the square wave residual stress field results.

4. Toughness enhancement and inferences

The unit-function, $g(t/L)$, associated with the various residual stress fields defined in Equations 8a–e are shown in Figs 4–7 as a function of the relative location, t/L, of the tip of the semi-infinite crack with respect to the periodicity of the residual stress field. In interpreting the results in these figures, note that negative values of the unit-function, $g(t/L)$, is associated with shielding of the semi-infinite crack under mode I loading, whereas positive values of $g(t/L)$ implies the residual stress field actually reduces the maximum

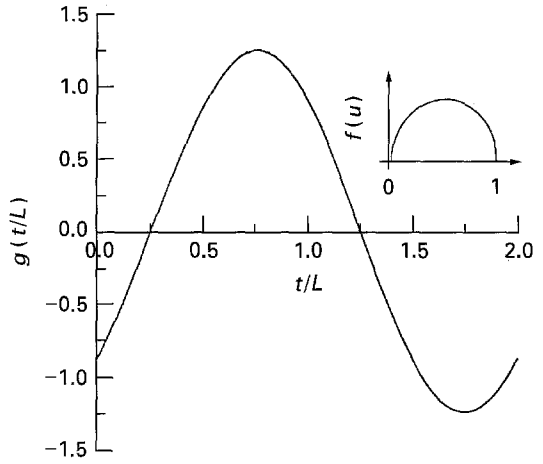

Figure 4 The sine wave unit-function as a function of crack-tip location.

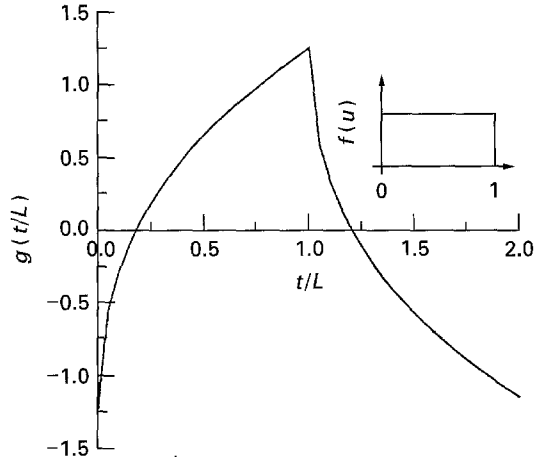

Figure 5 The square wave unit-function as a function of crack-tip location.

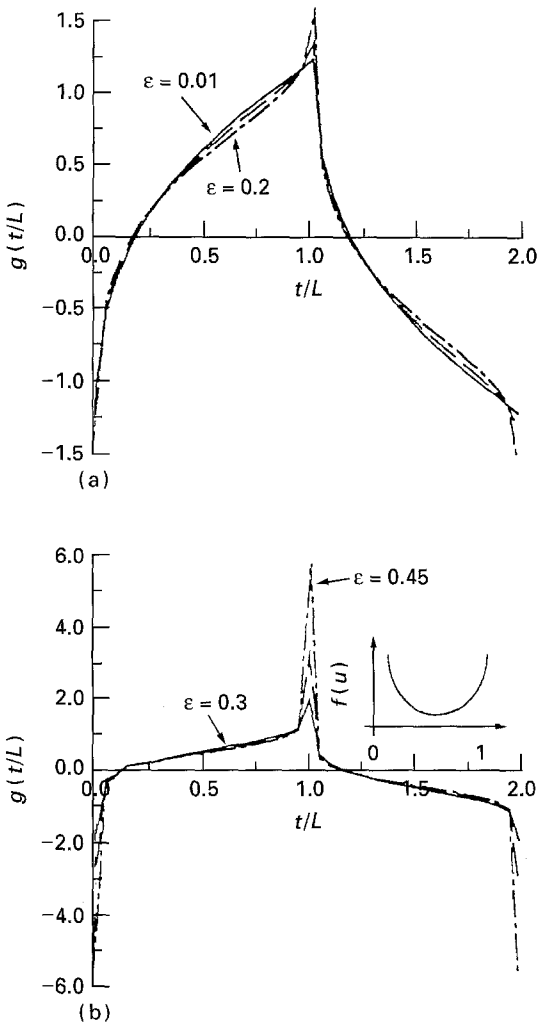

Figure 6 The algebraically singular unit-function as a function of crack-tip location: (a) for low values of the singularity parameter, ε, (b) for high values of the singularity parameter, ε.

load the cracked system can sustain. Figs 4 and 5 show the results for the two non-singular residual stress fields. The results for the algebraically singular fields are presented in Fig. 6 via two plots to highlight better the influence of the singularity parameter, ε, on toughness enhancement. The logarithmically singular fields results are presented in Fig. 7, where the dashed-line curve corresponds to value of the elastic anisotropy factor $\eta = 1/2^{1/2}$, while the solid-line curve corresponds to $\eta = 2^{1/2}$.

The most significant features of the results presented in Figs 4–7 are the minimum values of $g(t/L)$ and where they occur. In Table I the minimum values, $g_m(t/L)$, and the corresponding locations, $(t/L)_m$, for the various residual stress fields are listed. In addition, values of $g_m(t/L)$ are listed for the logarithmically singular residual stress fields specified by Equations 10a and b. With the exception of the sine wave residual stress field, maximum toughening of the semi-infinite crack occurs when the crack is at the verge of entering a residually tensile region corresponding to $(t/L)_m = 0$. This general trend, while counter-intuitive, follows from the observation that maximum toughening corresponds to weighting of the integral in Equation 6 in a manner which favours the presence of

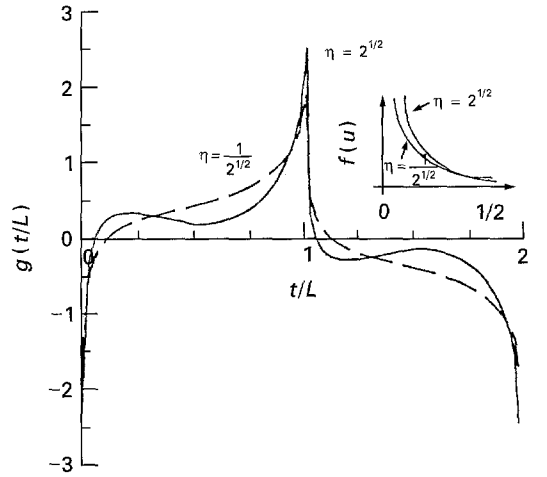

Figure 7 The logarithmically singular unit-function as a function of crack-tip location for two cases of the elastic anisotropy factor, η.

residual compressive stress adjacent to the crack tip in the crack-wake region. Deviation of the location of maximum toughening, $(t/L)_m$, for the sine wave residual stress field from the current trend is due to the fact that the minimum value of the sine wave function does not occur at the tension–compression cross-over point of the sine wave function.

TABLE I Minimum values of the unit function $g(t/L)$ and the corresponding crack-tip location, t/L

Residual stress		$(t/L)_m$	$g_m(t/L)$	
Sine		1.75	-1.25	
Square		0	-1.20	
Algebraically singular	$\varepsilon = -0.01$	0	-1.20	
	$\varepsilon = -0.1$	0	-1.32	
	$\varepsilon = -0.2$	0	-1.52	
	$\varepsilon = -0.3$	0	-1.94	
	$\varepsilon = -0.4$	0	-3.2	
	$\varepsilon = -0.45$	0	-5.7	
Logarithmically singular	$\eta = 2^{1/2}$	0	-2.45[a]	-0.98[b]
	$\eta = 1/2^{1/2}$	0	-1.85[a]	-0.98[b]

[a]Based on Equation 9.
[b]Based on Equations 10a and b.

Evidently, the sine and square wave residual stress fields are equally effective in shielding the semi-infinite crack from the applied load, with maximum toughening corresponding to values of the unit-function, $g_m(t/L)$, in the range $1.2 \leq g_m(t/L) \leq 1.25$. The algebraically singular fields provide a greater degree of toughening than the non-singular fields, even for relatively low values of the singularity parameter ε. For value of the singularity parameter $\varepsilon \leq -0.01$ the square wave residual stress field results are recovered. Minimum values of the unit-function, $g_m(t/L)$, for the logarithmically singular residual stress fields are approximately 1.6–2.1 times higher than the corresponding non-singular residual stress field values.

Toughness enhancement associated with a residual stress field, for a given value of the average residual stress, σ_0, is thus seen to depend strongly on the spatial variation function, $f(u)$, of the residual stress field. Among the family of residual stress fields considered in Equations 8a–e, the singular residual stress fields may, in fact, be the more realistic representations of the residual stress distribution within brittle polycrystalline materials [6]. Evidently, these singular fields provide a much greater degree of toughening than non-singular fields under equivalent value of σ_0. Comparing the results for the two cases of logarithmically singular residual stress that represent a wide range of grain-sized elastic anisotropy mismatches, deviation from elastic isotropy ($\eta = 1$) over the stated range of η values results in an approximate 14% difference in the minimum value of the unit-function $g_m(t/L)$. To the degree that the two cases of elastic anisotropy assumed in this study cover a reasonable range of actual material property, toughness enhancement due to residual stress is seen to depend weakly on the degree of elastic anisotropy within individual grains of a polycrystalline material.

Evaluation of the toughening ratio, Λ, in Equation 7 that is achievable with the various residual stress fields for a specific polycrystal requires knowledge of the average value of the residual stress, σ_0, the distribution function, $f(x)$, length of the average periodicity, $2L$, and the intrinsic toughness, K_m, of the polycrystal. Sample results for toughness enhancement achievable for a single-phase polycrystal is estimated in the next section under the assumption of intergranular fracture. It is believed that these results provide a reference estimate of the toughening achievable in polycrystalline ceramics due to residual stress effects in the absence of microcracking.

5. Sample results for a single-phase polycrystal

The residual stress field in the polycrystal is modelled by the logarithmically singular residual stress fields in Equations 8a–e. The residual stress field periodicity of length $2L$ is now identified with twice the average grain diameter of the polycrystal, consistent with both the periodicity assumed by Tvergaard and Hutchinson [6] and with the assumption that zero average residual stress occurs over a relatively small area. The reference residual stress, σ_0, is evaluated assuming

$$\sigma_0 = E\Delta\omega\Delta T \tag{12}$$

with Young's modulus $E = 400 \times 10^9\ \mathrm{N\,m^{-2}}$, difference between maximum and minimum thermal expansion coefficients $\Delta\omega = 7.4 \times 10^{-7}$ and difference between processing temperature and room temperature being $\Delta T = 1500\,^{\circ}\mathrm{C}$ [8]. Let $G_m = 2\ \mathrm{J\,m^{-2}}$ be the critical energy release rate associated with the grain boundary between individual grains and $\nu = 0.2$ be the corresponding value of the Poisson's ratio. The intrinsic toughness of the grain boundary is then approximately $K_m = 0.91\ \mathrm{MPa\,m^{1/2}}$. Note that both of the logarithmically singular residual stress fields considered in Equations 8d and e result in minimum value of the unit-function $g_m(t/L) \cong -1$. Substitution of the above values into Equation 12 with $g_m(0) = -1$ yields minimum values of the stress intensity factor contribution due to residual stress effects. These minimum values range from $K_r/K_m = -0.34$ for a very fine grain polycrystal with a mean grain size of 0.5 μm to $K_r/K_m = -2.17$ for a polycrystal with a mean grain size of 20 μm. Corresponding to these values of K_r/K_m are values of maximum toughening ratio that range from $(\Lambda)_m = 1.34$ to $(\Lambda)_m = 3.17$. The assumption of a different number of grains within each residual stress period of length $2L$ can be readily incorporated into the toughness calculation presented above through Equation 7.

Comparison with experimental data [8–11] indicate that the predicted maximum toughness values, although the outcome of a highly idealized model, are within the range of reported values for some ceramic systems. However, there is experimental evidence [8–10] that, in addition to residual stress effects of the type considered in this study, crack bridging by uncracked grains and grain-interlocking effects also serve as toughening mechanisms in polycrystalline ceramics. Nonetheless, the above estimate of toughness enhancement demonstrates the potential for substantial toughening in polycrystalline ceramics due to residual stress effects in the absence of microcracking.

Acknowledgement

This work was performed while the author was a graduate student at Harvard University. The mentorship of Professor John W. Hutchinson is gratefully acknowledged.

References

1. J. W. HUTCHINSON, *Acta Metall.* **35** (1987) 1605.
2. J. A. KUSZYK and R. C. BRADT, *J. Am. Ceram. Soc.* **56** (1973) 420.
3. A. G. EVANS, *Acta Metall.* **26** (1978) 1845.
4. D. R. CLARKE, *ibid.* **28** (1980) 913.
5. R. W. RICE, R. C. POHANKA and W. J. Mc DONOUGH, *J. Am. Ceram. Soc.* **63** (1980) 703.
6. V. TVERGAARD and J. W. HUTCHINSON, *ibid.* **71** (1988) 157.
7. H. TADA, P. C. PARIS and G. R. IRWIN, "Handbook for stress analysis of cracks", 2nd Edn (Del Research, 1985).
8. M. V. SWAIN, *J. Mater. Sci. Lett.* **5**, (1986) 1313.
9. P. L. SWANSON, C. J. FAIRBANKS, B. R. LAWN, Y. W. MAI and B. J. HOCKEY *J. Am. Ceram. Soc.* **70** (1987) 279.
10. G. VEKINIS, M. F. ASHBY and P. W. R. BEAUMONT, "Direct Observation of Fracture and the Damage Mechanisms of Ceramics", Cambridge University Report CUED/C-MATS/TR 148 (1988).
11. S. W. FREIMAN, *Ceram. Bull.* **67** (1988) 392.

Received 15 April 1994
and accepted 22 March 1995